Highlighting the effect of amyloid beta assemblies on the mechanical properties and conformational stability of cell membrane

Highlighting the Effect of Amyloid Beta Assemblies on the Mechanical Properties and Conformational Stability of Cell Membrane

Gianvito Grasso[1*], Chiara Lionello[2], and Filip Stojceski[1]

[1] Istituto Dalle Molle di studi sull'Intelligenza Artificiale (IDSIA), Scuola Universitaria Professionale della Svizzera italiana (SUPSI), Università della Svizzera italiana (USI), Centro Galleria 2, Manno, CH-6928, Switzerland.

[2] Department of Applied Science and Technology, Politecnico di Torino, Corso Duca degli Abruzzi 24, 10129 Torino, Italy

Abstract

Alzheimer disease (AD) is the most common cause of dementia, characterized by a progressive decline in cognitive function due to the abnormal aggregation and deposition of Amyloid beta (Aβ) fibrils in the brain of patients. In this context, the molecular mechanisms of protein misfolding and aggregation that are known to induce significant biophysical alterations in cells, including destabilization of plasma membranes, remains partially unclear. Physical interaction between the Aβ assemblies and the membrane leads to the disruption of the cell membrane in multiple ways including, surface carpeting, generation of transmembrane channels and detergent-like membrane dissolution. Understanding the impact of amyloidogenic protein in different stages of aggregation with the plasma membrane, plays a crucial role to fully elucidate the pathological mechanisms of AD. Within this framework, computer simulations represent a powerful tool able to shed lights on the interactions governing the structural influence of Aβ proteins on biological membrane. In this study, molecular dynamics (MD) simulations have been performed in order to characterize how POPC bilayer conformational and mechanical properties are affected by the interaction with $A\beta_{11-42}$ peptide, oligomer and fibril.

Keywords: Aβ, amyloid oligomer, amyloid beta, amyloid peptide, Alzheimer Disease, molecular dynamics, membrane destabilization, membrane fibril interaction, membrane thickness, area per lipid, order parameter, bending modulus, computational modelling, gromacs.

*Corresponding Author: gianvito.grasso@idsia.ch

Tel.: +41 (0)58 666 65 68

Introduction

Alzheimer's disease (AD) is a neurodegenerative disorder that cause irreversible loss of neurons, principally in the cortex and hippocampus. The primary neurotoxic species that causes Alzheimer's disease are small assemblies of amyloid β (Aβ) peptide [1]. The mechanism by which AD develops is not clear and there are not treatments able to slow or stop damage or loss of neurons. There are four principal hypothesis that try to explain AD onset: cholinergic [2], tau [3], amyloid cascade [4], and vascular [5], recently developed. The amyloid cascade is the most accredited hypothesis and consider the deposition of amyloid β plaques around neurons as the principal cause of the irreversible neuronal damage and memory loss. Aβ peptide is product from cleavage of the Amyloid Precursor Protein (APP) by α-, β- and γ-secretase [6]. There are two principal type of Aβ peptide, one constituted by 40 residues ($A\beta_{40}$), which accounts for 90% of secreted Aβ, and a less prevalent type constituted by 42 residues ($A\beta_{42}$)[7]. The stability of these structures is strongly related with the progression and severity of the disease, pushing the scientific community to huge efforts in order to characterize the molecular stability of amyloid aggregates and discover novel drugs [8–11]. However, $A\beta_{42}$ is the most toxic specie which is characterized by a polymorphic nature [12] and tends to aggregate in more rapidly way [13]. In detail, $A\beta_{40}$ can assume only a U-shaped structure instead of $A\beta_{42}$ that can adopt both U- and S-shaped structure [14]. Recent studies demonstrate that the S-shaped $A\beta_{42}$ is the most compact and stable specie [10,15,16].

Amyloid beta assemblies tend to interact with cell membranes. The association and the interaction of amyloid oligomers with lipid bilayer produce toxic effects on the normal cell functions and activities. Physical interaction between the peptide and the membrane leads to the disruption of the cell membrane in different ways, e.g. carpeting on the surface, penetrating in the cell membrane causing transmembrane channels, causing detergent-like membrane dissolution [17–20]. Ionic homeostasis, membrane leakage and cell toxicity are due to the disruption of the cell membrane, that causes the penetration of small molecules and ions inside the cell [21]. Changes in these interactions are due to the bilayer composition, e.g. different types of lipids and the percentage of cholesterol [22]. In this connection, a molecular level understanding of the interactions governing the structural influence of Aβ on biological membrane represents an important research advance.

Several studies have investigated the interaction between amyloid protein, i.e. monomer and small oligomer, and different type of bilayer. Studies reported here analyse the effects of amyloid protein on POPC bilayer. *Xiang et al.*[23] found that oligomers with more than two peptides tend to modify the lipid bilayer by generating water channels, besides, with the increasing of the number of peptides the free energy of penetration tends to decrease. In another work [24] authors conclude that in case of carpeting of amyloid peptide on the membrane, the latter undergo perturbation becoming more gel-like and rigid modifying area per lipid and order parameter. Nevertheless, since POPC is a zwitterionic bilayer, both the membrane and the protein inserted in it tend to remain stable during MD simulations [25,26]. Other MD studies demonstrate that the insertion of Aβ oligomers into explicit solvated lipid bilayer is not spontaneous due to high energy barrier [21]. However, once an oligomer is inserted into the membrane, it causes a thinning of the bilayer and this consequences increase with the assembly dimension [27].

Jang et al. have simulated a pore formation starting from small Aβ40 fibril, showing local thinning, membrane disruption and local increasing of the surface pressure as a consequence of Aβ40 insertion into cell membrane. Another consequence of Aβ association with cell membrane is cytotoxic effect due to an increase in membrane fluidity [28].

Starting from these observations, MD simulations were employed to study and analyse the effects of $A\beta_{11\text{-}42}$ protein on POPC bilayer from the conformational and mechanical point of view. In particular, the main focus of this work is to evaluate the influence of the amyloidogenic protein in different stages of aggregation on the plasma membrane.

Material and Methods

Aβ peptide in water

The $A\beta_{11\text{-}42}$ peptide model was extracted from the Protein Data Bank (PDB ID: 1IYT [29]). The first system was composed by the $A\beta_{11\text{-}42}$ peptide placed in a triclinic box, with a distance of 2 nm from the edge of the box to respect the minimum image condition. The obtained system was solvated with explicit water and Na-Cl ions were added in order to obtain a concentration of 0.15 M. After an energy minimization protocol, NVT and NPT equilibration, 300 ns of non-restrained MD simulation was performed.

Aβ oligomer in water

Five Aβ peptides representative structure was extracted from the last 100 ns of 300ns long MD and were placed randomly in a triclinic box. Each monomer was separated from the other and from the edge of the box at least by 1.2 nm to avoid long-range interaction. The system was solvated with water and the NaCl salt concentration was fixed at 0.15 M. After an energy minimization protocol, NVT and NPT equilibration, 500 ns of non-restrained MD simulation was performed, extracting a conformation of the $A\beta_{11\text{-}42}$ oligomer following the procedure of another work [30].

Aβ fibril in water

The 5 chain $A\beta_{11\text{-}42}$ fibril model was extracted from the Protein Data Bank (PDB ID: 2MXU [31]). The first system was composed by the $A\beta_{11\text{-}42}$ fibril placed in a triclinic box, with a distance of 1.2 nm from the edge of the box to respect the minimum image condition. The obtained system was solvated with explicit water and Na-Cl ions were added at concentration of 0.15 M. After an energy minimization protocol, NVT and NPT equilibration, 300 ns of non-restrained MD simulation was performed.

Aβ in membrane

To evaluate the impact of amyloid β assemblies on the membrane, a peptide, a 5-mer oligomer and a 5-mer fibril were inserted into a POPC bilayer using CHARMM-GUI software [32–34]. A lipid bilayer of 14 nm x 14 nm was created, adding 2 nm layer of water on both side of the membrane. The ions concentration was fixed at 0.15 M, obtaining systems between 140000 and 170000 particles.

Peptide and oligomer were inserted into the bilayer with random orientation, while, in order to create different replicas, the fibril was oriented in a different way for every system (Supporting Information-S.1). A POPC bilayer was created with the same dimensions as above, except for the 1 nm of water thickness. This membrane system was used to compare the results obtained from the above-mentioned membrane protein systems.

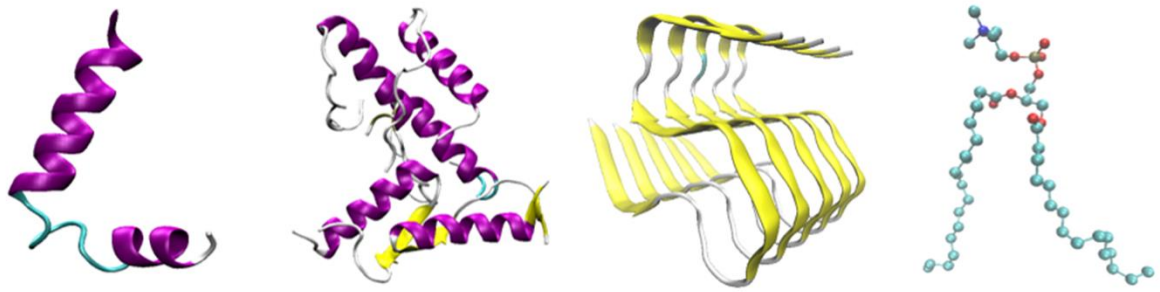

Figure 1 – Visualization of the systems' main component. Starting from the left are represented the peptide, the oligomer, the fibril and a POPC phospholipid

Simulation Setups

CHARMM36 [35] forcefield was considered to model protein topology, and the system was solvated with explicitly modelled TIP3P water [36]. Each systems were subjected to energy minimization by the steepest descent algorithm [37]. Subsequently an NVT ensemble for 100 ps at 300 K by means V-rescale algorithm [38] and time constant of 0.1 ps. The correct density of 1 atm was achieved with 100 ps NPT equilibration using Berendsen algorithm [39] with a semi-isotropic coupling type.

The MD production has been has been performed using Nose-Hoover [40] (T = 300 K) and Parrinello-Rahman [39] (P = 1 atm) were used as temperature and pressure coupling. Electrostatic was calculated using Particle Mesh Ewald (PME) algorithm [41] and Van der Waals with the cut-off of 1.2 nm. Periodic boundary conditions were applied in all three dimensions.

Simulations were performed using GROMACS software package, version 5.1.4 [42]. Trajectories were extracted every 20 ps of simulation and the Visual Molecular Dynamics (VMD) package is used to display the simulated systems. All the results are calculated on the last 20 ns for each system.

Trajectory analysis

To analyse the membrane's effects on the protein, Root Mean Square Fluctuation (RMSF), Solvent Accessible Surface Area (SASA) and an order parameter were implemented.

To analyse the conformational properties of the membrane, area per lipid (APL) and bilayer thickness were obtained using GridMAT-MD tool [43] with 100x100 grid points.

While, the lipid order parameter (ρ_r) was implemented to study the orientation of POPC lipids. It was calculated using the following equation:

$$\rho_r = \left\langle \frac{3cos^2\theta - 1}{2} \right\rangle$$

where θ is the angle between the lipid identifier vector (see Supporting Information-S.2) and z-axis, normal to the membrane. The angle brackets indicate the time average over all atoms located inside a certain circular crown. Circular crowns were 1 nm thick and were determinate on function of the distance from the protein. The order parameter varies between 1, indicating full order along the interface normal, and -1/2, denoting full order along the perpendicular to the interface normal, while 0 means no lipidic order.

The membrane bending modulus (K_c) was calculated with the method explain in a *Khelashvili et al.* work [44], which suggest a heuristic approximation for calculating the monolayer bending modulus from MD trajectories. The bending modulus is correlated with the ability of the lipid membrane component to change orientation respect each other. This lipid ability is described by the splay angle (α, between 0° and 90°) which is related to the splay module χ_{12}. The potential mean force ($PMF(\alpha)$) was obtained from the probability distribution $P(\alpha)$ of the splay angle:

$$PMF(\alpha) = -k_B T ln\left[\frac{P(\alpha)}{P_0(\alpha)}\right]$$

where $P_0(\alpha) = \sin(\alpha)$ is the probability distribution of a hypothetical non-interacting particle system [45], k_B is the factor of Boltzmann and T is the temperature of the system. Fitting the $PMF(\alpha)$ data with a quadratic function permits to obtain the tilt module χ and the splay module χ_{12}. Then:

$$\frac{1}{k_m} = \frac{1}{\phi_{total}} \sum_{\langle i,j \rangle} \frac{\phi_{ij}}{\chi_{12}^{ij}}$$

Where χ_{12}^{ij} is the splay modulus for the *ijth* pair type, $\phi_{ij}$is the number of near-neighbouring *ij* encounter pairs, obtained directly from MD trajectories, and $\phi_{total} = \sum_{ij} \phi_{ij}$ represents the total number of encounters in the simulation for all possible pairwise contributions $\langle i, j \rangle$ for which the splay is calculated. Since the bilayer was composed by only POPC, the splay module corresponds to k_m.

Using the heuristic approximation, the bilayer bending modulus was:

$$K_C = 2k_m$$

Bending modulus has been calculated also as function of the distance from the protein, 2 nm thick circular crowns were isolated. The value obtained are reported as function of the mean radius.

Results

The results are divided in two main sections, the first regarding the conformation of $A\beta_{11\text{-}42}$ protein in water and in membrane environments and the second regarding the effects of $A\beta_{11\text{-}42}$ protein on the POPC bilayer. A visual inspection of the molecular systems at the end of each MD simulation is shown in Figure 2, while a visual inspection of the molecular systems in the initial configuration is represented in supporting information-S.3.

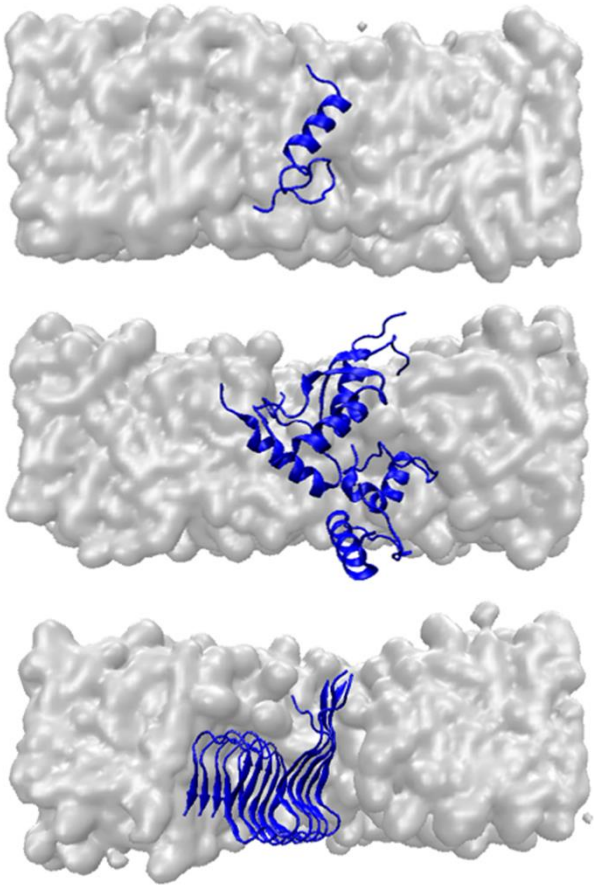

Figure 2 - Representation of the final states for each system studies. From the top to the bottom respectively: the peptide, the oligomer and the fibril embedded in the POPC bilayer.

Conformation of $A\beta_{11-42}$ protein in water and in membrane

$A\beta_{11-42}$ protein conformation analysis is a first stage of knowledge suitable to spot difference in the effects of the peptide, oligomer and fibril on the membrane. As first analysis, protein fluctuations are evaluated with Root Mean Square Fluctuation (RMSF) (Figure 3). In all cases, protein in water fluctuates more than the protein in membrane, as expected. In detail, higher RMSF difference is highlighted for the peptide (Figure 3A) and the oligomer (Figure 3B). Instead, the fibril shows a more stable behaviour, reporting differences only on the C-terminal part, from residue V36, because of the exposure to the solvent (Figure 3C). Nonetheless, the fluctuation of the C-terminal part when the fibril is in a solvent environment is in agreement with recent findings [15]. Furthermore, the Solvent Accessible Surface Area (SASA) per residue is calculated to shed lights on the tendency of each residue of exposing itself in the solvent and membrane environments (Figure 3). Proteins tend to have the same behaviour both in water and in membrane. Observing Figure 3D, which is referred to the peptide, some differences can be noted for residues F20, I32 and I41 where values are higher for the protein in membrane. In case of oligomer (Figure 3E), a difference can be noted between residues 31 and V36 where values are higher

for the assembly in membrane. In Figure 3F, the Aβ fibril shows the same behaviour in water and in membrane.

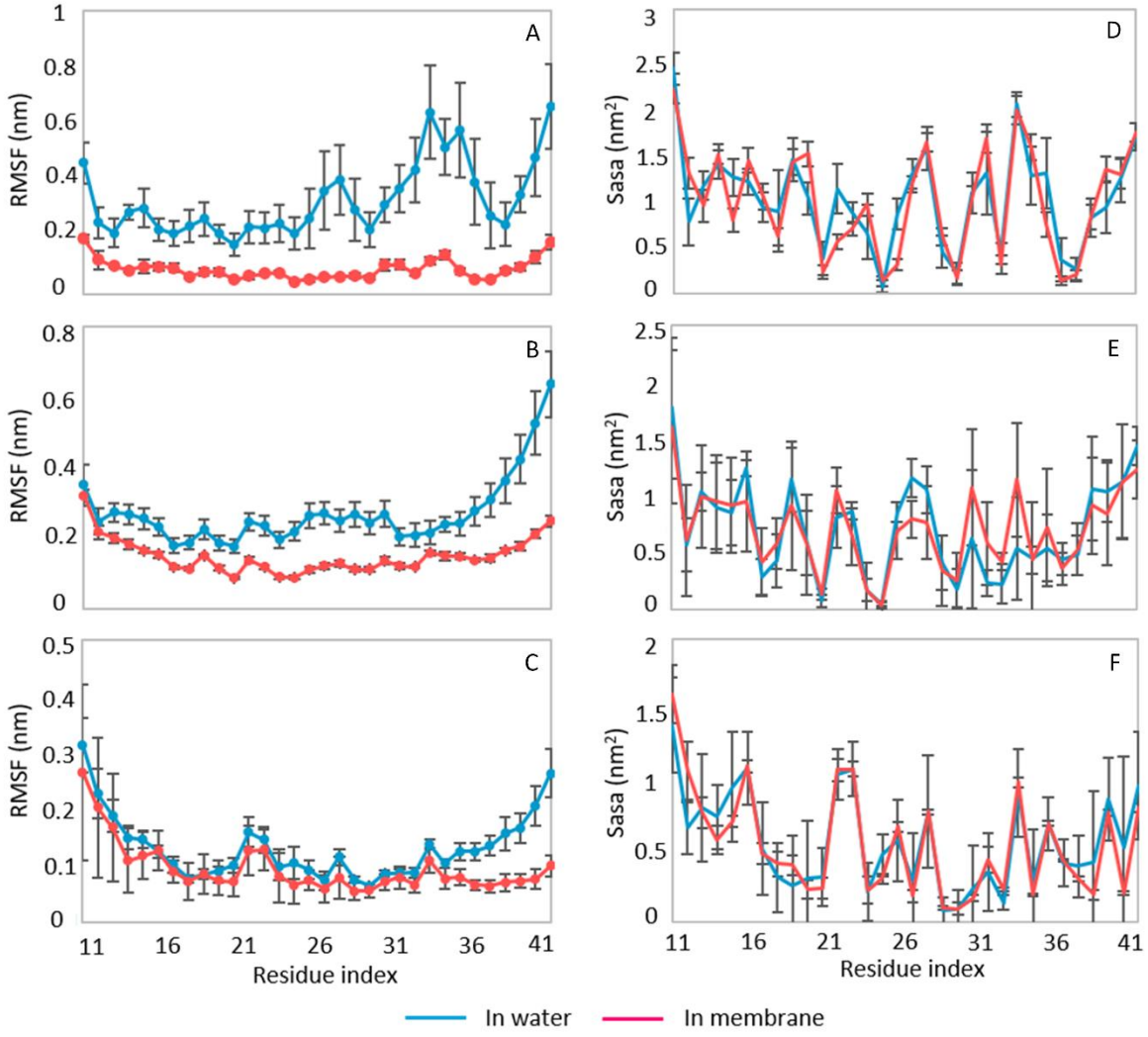

Figure 3 – Representation of protein fluctuations using Root Mean Square Fluctuations (RMSF) and protein solvent Accesible Surface Area (SASA). The pictures show respectively: **A**) RMSF for Aβ peptide both in water and in membrane, **B**) RMSF for the oligomer both in solution and inserted into POPC bilayer, **C**) RMSF for the fibril both in water and in membrane. is calculate, **D**) SASA for peptide both in water and in membrane, **E**) SASA for oligomer in water and in membrane and **F**) SASA for fibril both in water and in membrane.

The mean value and standard deviation of inter-chain contact area are calculated and reported in Figure 4 for the oligomer and the fibril. This graph highlights the differences between the Aβ fibril, that is more compact, characterized by a high contact area and low standard deviation, while the Aβ oligomer tends to expose more the hydrophilic part as it is characterized by low mean value and high standard deviation. The outcome of this analysis means that the fibril remains stable and compact in membrane unlike the oligomer that is disordered and more exposed to the solvent.

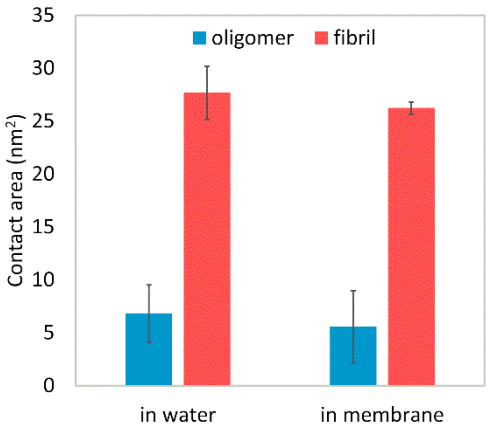

Figure 4 – Protein contact area. The fibril is characterized by a high contact area and low standard deviation, while the oligomer is characterized by low mean value and high standard deviation, as it tends to expose the hydrophilic part.

Effects on POPC bilayer by $A\beta_{11\text{-}42}$ protein

Understanding the impact of amyloidogenic protein in different stages of aggregation with the plasma membrane plays a crucial role to fully elucidate the pathological mechanisms of AD. To address this point, several analyses have been performed in order to evaluate membrane conformational and mechanical features of the membrane complexed with the amyloidogenic proteins. Firstly, APL parameter has been calculated obtaining a value for membrane alone of 61.6 ± 0.2 Å^2, which is considered as reference in calculation of percentage variation of peptide, oligomer and fibril systems (Figure 5A). This value is in agreement with both experimental and simulation works 64.0 ± 1.5 Å^2 [24,46–48]. After the insertion of the protein in the membrane, there is an increase in APL value for peptide, oligomer and fibril systems. In particular, with peptide there is an increase of about 2.0% (62.8 ± 0.7 Å^2), with oligomer of 8.2% (66.7 ± 0.6 Å^2) and with fibril of 8.6% (66.9 ± 0.7 Å^2). It is reasonable to hypothesize that assemblies tend to destabilize the membrane more than the peptide.

Further consequence of insertion of Aβ protein into lipid bilayer may be the variation of bilayer thickness. In this framework, membrane thickness parameter has been calculated obtaining a value for membrane alone of 4.02 ± 0.02 nm, which is considered as reference in calculation of percentage variation of peptide, oligomer and fibril systems (Figure 5B). In this context, the value with peptide remains almost unchanged as only decrease by 0.9% (3.99 ± 0.04), instead oligomer and fibril have a reduction of the value by 3.9%, resulting is a thickness values of respectively, 3.86 ± 0.02 nm and 3.86 ± 0.05 nm.

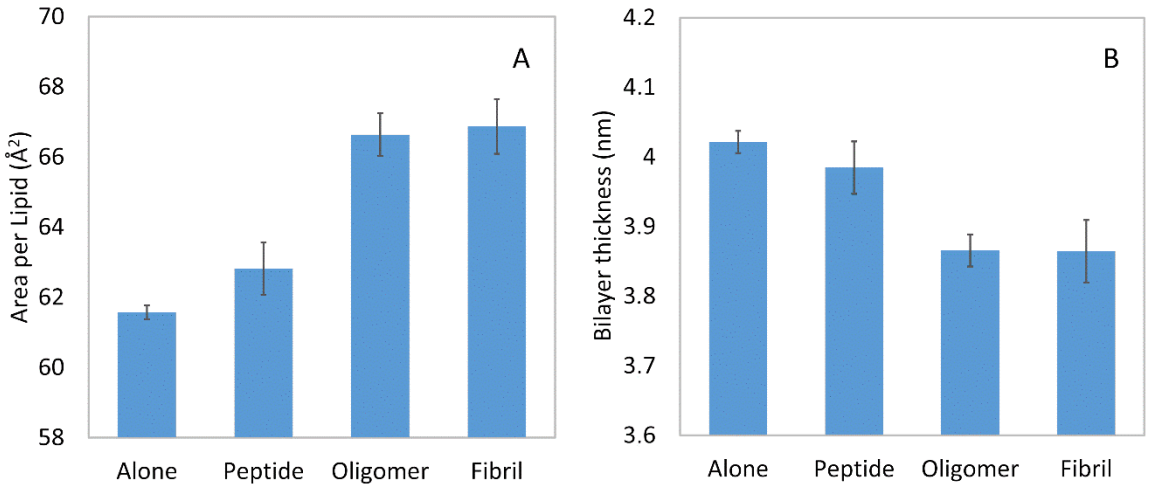

Figure 5 – (A) Area per lipid values for membrane alone, peptide, oligomer and fibril systems. (B) Bilayer thickness values for membrane alone, peptide, oligomer and fibril systems.

Another important conformational feature of the membrane phospholipids is the order parameter, which is calculated as function of the POPC distance from the protein (Figure 6). The distance in case of membrane alone is referred to the centre of the bilayer. To obtain order parameter as function of the distance, 1 nm thick circular crown is taken into account, and the value is shown in correspondence of the mean radius. Figure 6 highlights how in proximity of the protein, the bilayer is less ordered than the membrane alone, especially in the case of membrane with oligomer and fibril. In particular, it can be noted that the order parameter is restored when the distance from the assemblies increases, namely over 4 nm from the proteins' centre of mass. Instead, in the case of membrane with peptide, the order parameter does not undergo major changes.

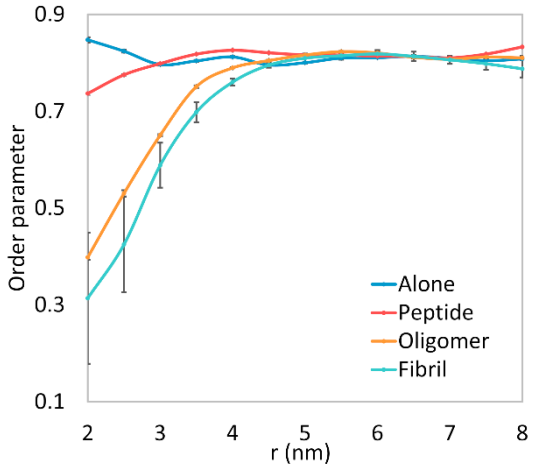

Figure 6 - A) represents of the order parameter as function of the distance from the centre of mass of the protein. In case of only membrane, the distance is referred to the centre of the bilayer. 1nm thick circular crown are isolated and the order parameter calculated is represented in correspondence of the mean radius.

Finally, membrane mechanical properties are evaluated by an estimation of the bending modulus (Figure 7), as previously done in literature [49–51]. Figure 7A shows the bending modulus reported as function of the distance from the inserted protein. It has been computed considering 2 nm thick circular crown and reporting the value in correspondence of the mean radius. The bending modulus value for

membrane alone is 21.5 ± 0.4 k_BT. In the region near assemblies, namely at 2 nm from Aβ protein centre of mass, is observable a drastically decreased of the bending modulus reaching respectively, 13.2± 0.4 k_BT for the oligomer and 12.7± 0.4 k_BT for the fibril. These findings are in agreement with the *Borro et al*. [52] scientific group results, which highlight how the bending modulus of 23.6±1.9 k_BT and 21.5±1.3 k_BT for DOPC membrane calculated at pH respectively of 4 and 2, is strongly affected after insertion of prefibrillar species and fibrils, reducing it to 11.3 ± 0.9 k_BT and 14.5±1.1 k_BT respectively. Figure 7B shows the average of first 4.5 nm referred to the Aβ protein centre of mass, in which is highlighted the major bending modulus decrease, especially for the oligomer and fibril. Furthermore, it must be noted that beyond the distance of 4.5 the membrane with peptide is able to restore the bending modulus value close to the membrane alone, while in the case of oligomer and fibril the bending modulus value reach a plateau close to 18 k_BT. In this context, this results in a long-range impairment of the mechanical plasmatic membrane properties, which may promote structural destabilization processes.

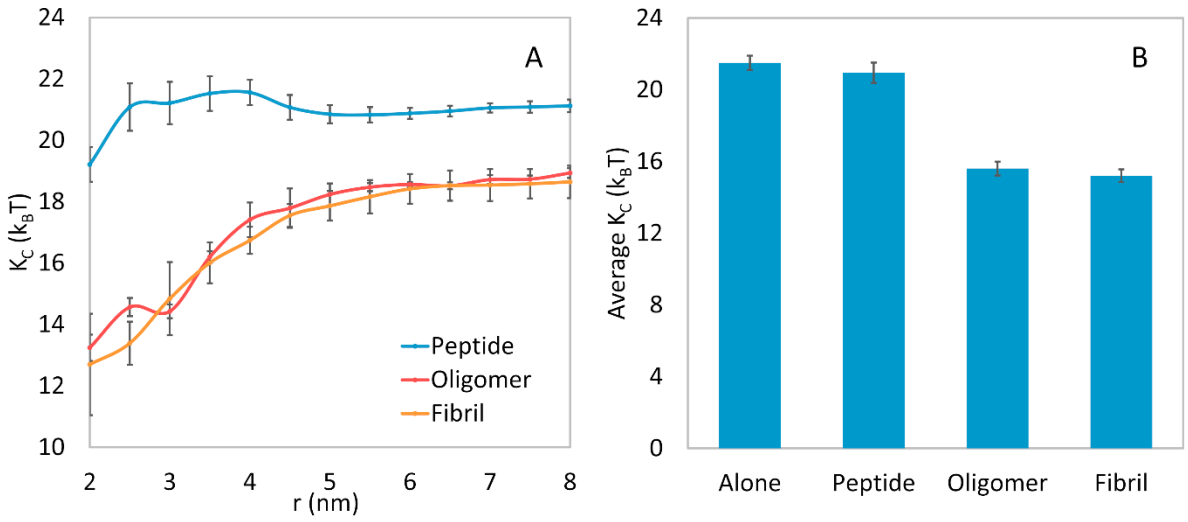

Figure 7 – (A) Bending modulus variation as function of the distance fom the centre of mass of the protein and (B) average bending modulus of first 4.5 nm from the aggregates centre of mass. Assemmblies tend to destabilize the bilayer more than the pepdite. In particular the major influences is found in first 4.5 nm from the aggregates centre of mass. Moving away from the amyloidogenic oligomer and fibril, bilayer mechanical properties are not restored to the reference value of membrane alone.

It is interesting to see that mechanical properties of the membrane are not affected by the interaction with the peptide, since no significant changes were observed. On the other hand, our data demonstrated how the membrane is destabilized by the presence of the Aβ assemblies. Within this framework, oligomer and fibril modify in a similar way the area per lipid and bilayer thickness but in different ways the tilt and splay angle. Moreover, variations in order parameter and bending modulus are strongly linked to the distance from the proteins' centre of mass.

Discussion

AD is a neurodegenerative disease that leads to a progressive deterioration of cognitive functions, characterized by an uncontrolled aggregation and deposition of Aβ plaques in the brain. The two principal isoforms of Aβ peptides is the $A\beta_{1-40}$, with 40 residues long chain and the more toxic $A\beta_{1-42}$, composed by 42-residues long chain [53]. Even if $A\beta_{1-42}$ is present in smaller quantity than $A\beta_{1-40}$, it is the main responsible of triggering the diffusive deposits [54]. Neuronal membrane destabilization after the interaction with different size of Aβ assemblies are common structural links among various neurodegenerative diseases [55]. In this connection, Aβ is able to insert itself into the bilayer causing severe membrane damage [23,56]. The toxic influence of the misfolded proteins on the membrane depends on the phospholipids composition and the cholesterol percentage of the plasmatic membrane[57]. Moreover, the membrane composition plays also a crucial role in promoting the aggregation process of amyloidogenic peptides [58–61]. In this work the bilayer consists of only zwitterionic POPC phospholipids, because they constitute eukaryotic cell membrane and PC lipids are abundant in neuronal membrane [62].

In all the different simulated systems, the protein tends to stay embedded in the bilayer. This is compatible with what found by *Xiao et al*. [31], where their results shows that trimer and pentamer remain inside the membrane, differently to monomer and dimer. In this research, the peptide remains inside the membrane probably for the short duration of the simulation. The protein does not undergo changes if inserted into POPC bilayer. Other studies report the same conclusion and the main reason is because such lipids have zwitterionic characteristic and tend to not modify protein's properties [63,64].

Recent findings have raised the possibility that precursors to amyloid fibrils, such as low molecular weight oligomers and/or structured proto-fibrils, are the real pathogenic species, at least in neuropathic diseases like AD [65,66]. Within this context, the human and animal model brain tissue have shown the presence of Aβ oligomers in an AD-dependent manner [67–72]. The results of this work indicate that membrane undergoes in some modification, especially when the Aβ assemblies are embedded. Contrary to what happens in literature [24], there is an increase in area per lipid because some lipids tend to surround the protein moving toward the centre of the bilayer. However, an increase in APL is compatible with the decrease in bending modulus. Furthermore, the membrane fluidity increase after the Aβ association with membrane is another factor which increases the cytotoxicity and promote the cell apoptosis [28]. In literature has been ascertained that once oligomer is inserted into the membrane, it causes a thinning of the bilayer dependent on the size of the protein assembly [27]. In addition, the decrease in bilayer thickness is comparable with results from other works [73,74].

More interesting are the variation in order parameter and bending modulus. In case of bending modulus, results obtained for membrane alone are in agreement with literature 20.3 k_BT [73] and 24.6 ± 2.6 k_BT [75]. Variations in order parameter are observed also in other studies[24,25]. The trend of these properties shows that Aβ assemblies influence is enclosed in the first 4.5 nm from the proteins' centre of mass. Instead, beyond this radius the order parameter is recovered unlike the bending modulus that

reaches a plateau at a lower value respect the one for membrane alone, as if there were a long-range interaction of the protein.

Considering the recent findings, it has been demonstrated a strong causative link between conformational arrangements of Aβ assemblies and their neuronal toxicity [76–78], especially with regard to the high cytotoxicity of the Aβ oligomers if compared with other Aβ species [79–81]. The outcome of this work shows how both oligomers and fibrils are capable of destabilizing cell membranes from a conformational and mechanical point of view, which may be helpful in understanding the membrane experimentally demonstrated destabilization of Aβ assemblies [82–87].

Conclusion

Unveiling the reasons behind the toxicity of Aβ assemblies at different stages of the aggregation process plays a key role towards developing effective strategies against amyloidogenic pathologies as Alzheimer's and Parkinson's diseases. Within this framework, plasmatic membrane destabilization upon interaction with different Aβ-protein states is directly related to the progress of neurodegenerative disorders. In the present work molecular dynamics simulations have been applied to understand how amyloidogenic peptide, oligomer and fibril affect the cellular membrane from a conformational and mechanical point of view. In particular, oligomer and fibrils assemblies have been ascertained to influence the membrane thickness and area-per-lipid, suggesting a "thinning" of the phospholipids bilayer. In order to complete this picture, mechanical properties of the membrane will be tested in presence of oligomer and fibril aggregates. The results show that Aβ assemblies strongly affect the order parameter and bending modulus values, suggesting a "softening" of the plasmatic membrane. Further *in silico* and *in vitro* investigations regarding the interaction of Aβ species and membrane is of crucial importance in order to better understand the mechanisms of cell damage by amyloidogenic proteins.

Competing interests

The authors declare no competing interests

Acknowledgements

This work was supported by a grant from the Swiss National Supercomputing Centre (CSCS).

References

[1] C. Di Scala, N. Yahi, S. Boutemeur, A. Flores, L. Rodriguez, H. Chahinian, J. Fantini, Common molecular mechanism of amyloid pore formation by Alzheimer's β-amyloid peptide and α-synuclein, Sci. Rep. 6 (2016) 28781. doi:10.1038/srep28781.

[2] P. Davies, A.J.F. Maloney, Selective Loss of Central Cholinergic Neurons in Alzheimer'S Disease, Lancet. 308 (1976) 1403. doi:10.1016/S0140-6736(76)91936-X.

[3] R.D. Terry, The pathogenesis of Alzheimer disease: An alternative to the amyloid hypothesis, J. Neuropathol. Exp. Neurol. 55 (1996) 1023–1025. doi:10.1097/00005072-199655100-00001.

[4] J.A. Hardy, G.A. Higgins, Alzheimer's disease: The amyloid cascade hypothesis, Science (80-.). 256 (1992) 184–185. doi:10.1126/science.1566067.

[5] J.C. De la Torre, T. Mussivand, Can disturbed brain microcirculation cause Alzheimer's disease?, Neurol. Res. 15 (1993) 146–153. doi:10.1080/01616412.1993.11740127.

[6] D. Meleleo, A. Galliani, G. Notarachille, AβP1-42 incorporation and channel formation in planar lipid membranes: The role of cholesterol and its oxidation products, J. Bioenerg. Biomembr. 45 (2013) 369–381. doi:10.1007/s10863-013-9513-0.

[7] D.C. Bode, M.D. Baker, J.H. Viles, Ion channel formation by amyloid-β42 oligomers but not amyloid-β40 in cellular membranes, J. Biol. Chem. 292 (2017) 144–1413. doi:10.1074/jbc.M116.762526.

[8] F.L. Palhano, J. Lee, N.P. Grimster, J.W. Kelly, Toward the molecular mechanism(s) by which EGCG treatment remodels mature amyloid fibrils, J. Am. Chem. Soc. 135 (2013) 7503–7510. doi:10.1021/ja3115696.

[9] S. Muscat, F. Stojceski, A. Danani, Elucidating the Effect of Static Electric Field on Amyloid Beta 1–42 Supramolecular Assembly, J. Mol. Graph. Model. 96 (2020) 107535. doi:10.1016/j.jmgm.2020.107535.

[10] G. Grasso, M. Rebella, U. Morbiducci, J.A. Tuszynski, A. Danani, M.A. Deriu, The Role of Structural Polymorphism in Driving the Mechanical Performance of the Alzheimer's Beta Amyloid Fibrils, Front. Bioeng. Biotechnol. 7 (2019) 1–11. doi:10.3389/fbioe.2019.00083.

[11] S. Muscat, L. Pallante, F. Stojceski, A. Danani, G. Grasso, M.A. Deriu, The Impact of Natural Compounds on S-Shaped Aβ42 Fibril: From Molecular Docking to Biophysical Characterization, Int. J. Mol. Sci. 21 (2020) 2017. doi:10.3390/ijms21062017.

[12] M. Fändrich, J. Meinhardt, N. Grigorieff, Structural polymorphism of Alzheimer Aβ and other amyloid fibrils, Prion. 3 (2009) 89–93. doi:10.4161/pri.3.2.8859.

[13] J.L. Cummings, Alzheimer's disease, N. Engl. J. Med. 351 (2004) 56-67+110. doi:10.1056/NEJMra040223.

[14] W. Xi, W. Wang, G. Abbott, U.H.E. Hansmann, Stability of a Recently Found Triple-β-Stranded Aβ1-42 Fibril Motif, J. Phys. Chem. B. 120 (2016) 4548–4557. doi:10.1021/acs.jpcb.6b01724.

[15] G. Grasso, M. Rebella, S. Muscat, U. Morbiducci, J. Tuszynski, A. Danani, M.A. Deriu, Conformational dynamics and stability of u-shaped and s-shaped amyloid β assemblies, Int. J. Mol. Sci. 19 (2018) 571. doi:10.3390/ijms19020571.

[16] D.M.Á.V. Acosta, B.C. Vega, J.C. Basurto, L.G.F. Morales, M.C.R. Hernández, Recent advances by in silico and in vitro studies of amyloid-β 1-42 fibril depicted a S-shape conformation, Int. J.

Mol. Sci. 19 (2018). doi:10.3390/ijms19082415.

[17] O. Press-Sandler, Y. Miller, Molecular mechanisms of membrane-associated amyloid aggregation: Computational perspective and challenges, Biochim. Biophys. Acta - Biomembr. 1860 (2018) 1889–1905. doi:10.1016/j.bbamem.2018.03.014.

[18] R. Capone, F.G. Quiroz, P. Prangkio, I. Saluja, A.M. Sauer, M.R. Bautista, R.S. Turner, J. Yang, M. Mayer, Amyloid-β-induced ion flux in artificial lipid bilayers and neuronal cells: Resolving a controversy, Neurotox. Res. 16 (2009) 1–13. doi:10.1007/s12640-009-9033-1.

[19] A. Quist, I. Doudevski, H. Lin, R. Azimova, D. Ng, B. Frangione, B. Kagan, J. Ghiso, R. Lal, Amyloid ion channels: A common structural link for protein-misfolding disease, Proc. Natl. Acad. Sci. U. S. A. 102 (2005) 10427–10432. doi:10.1073/pnas.0502066102.

[20] J.R. Brender, U.H.N. Dürr, D. Heyl, M.B. Budarapu, A. Ramamoorthy, Membrane fragmentation by an amyloidogenic fragment of human Islet Amyloid Polypeptide detected by solid-state NMR spectroscopy of membrane nanotubes, Biochim. Biophys. Acta - Biomembr. 1768 (2007) 2026–2029. doi:10.1016/j.bbamem.2007.07.001.

[21] Y. Liu, B. Ren, Y. Zhang, Y. Sun, Y. Chang, G. Liang, L. Xu, J. Zheng, Molecular simulation aspects of amyloid peptides at membrane interface, Biochim. Biophys. Acta - Biomembr. 1860 (2018) 1906–1916. doi:10.1016/j.bbamem.2018.02.004.

[22] J.A. McLaurin, A. Chakrabartty, Characterization of the interactions of Alzheimer β-amyloid peptides with phospholipid membranes, Eur. J. Biochem. 245 (1997) 355–363. doi:10.1111/j.1432-1033.1997.t01-2-00355.x.

[23] N. Xiang, Y. Lyu, X. Zhu, G. Narsimhan, Investigation of the interaction of amyloid β peptide (11-42) oligomers with a 1-palmitoyl-2-oleoyl-sn-glycero-3-phosphocholine (POPC) membrane using molecular dynamics simulation, Phys. Chem. Chem. Phys. 20 (2018) 6817–6829. doi:10.1039/c7cp07148e.

[24] A.M. Brown, D.R. Bevan, Influence of sequence and lipid type on membrane perturbation by human and rat amyloid β-peptide (1–42), Arch. Biochem. Biophys. 614 (2017) 1–13. doi:10.1016/j.abb.2016.11.006.

[25] S.T. Ngo, H.M. Hung, K.N. Tran, M.T. Nguyen, Replica exchange molecular dynamics study of the amyloid beta (11-40) trimer penetrating a membrane, RSC Adv. 7 (2017) 7346–7357. doi:10.1039/c6ra26461a.

[26] C. Poojari, A. Kukol, B. Strodel, How the amyloid-β peptide and membranes affect each other: An extensive simulation study, Biochim. Biophys. Acta - Biomembr. 1828 (2013) 327–339. doi:10.1016/j.bbamem.2012.09.001.

[27] D.L. Parton, J.W. Klingelhoefer, M.S.P. Sansom, Aggregation of model membrane proteins, modulated by hydrophobic mismatch, membrane curvature, and protein class, Biophys. J. 101 (2011) 691–699. doi:10.1016/j.bpj.2011.06.048.

[28] R.P. Mason, R.F. Jacob, M.F. Walter, P.E. Mason, N.A. Avdulov, S. V. Chochina, U. Igbavboa, W.G. Wood, Distribution and fluidizing action of soluble and aggregated amyloid β- peptide in rat synaptic plasma membranes, J. Biol. Chem. 274 (1999) 18801–18807. doi:10.1074/jbc.274.26.18801.

[29] O. Crescenzi, S. Tomaselli, R. Guerrini, S. Salvadori, A.M. D'Ursi, P.A. Temussi, D. Picone, Solution structure of the Alzheimer amyloid β-peptide (1-42) in an apolar microenvironment: Similarity with a virus fusion domain, Eur. J. Biochem. 269 (2002) 5642–5648. doi:10.1046/j.1432-1033.2002.03271.x.

[30] A.M. Brown, D.R. Bevan, Molecular Dynamics Simulations of Amyloid β-Peptide (1-42): Tetramer Formation and Membrane Interactions, Biophys. J. 111 (2016) 937–949. doi:10.1016/j.bpj.2016.08.001.

[31] Y. Xiao, B. Ma, D. McElheny, S. Parthasarathy, F. Long, M. Hoshi, R. Nussinov, Y. Ishii, Aβ(1-42) fibril structure illuminates self-recognition and replication of amyloid in Alzheimer's disease, Nat. Struct. Mol. Biol. 22 (2015) 499–505. doi:10.1038/nsmb.2991.

[32] X. Cheng, J.B. Klauda, S. Jo, D.A. Case, J.C. Jeong, J.A. Lemkul, V.S. Pande, J.M. Swails, Y. Qi, P.K. Eastman, W. Im, C.L. Brooks, J. Lee, S. Wei, A.D. MacKerell, M.S. Yeom, J. Buckner, CHARMM-GUI Input Generator for NAMD, GROMACS, AMBER, OpenMM, and CHARMM/OpenMM Simulations Using the CHARMM36 Additive Force Field, J. Chem. Theory Comput. 12 (2015) 405–413. doi:10.1021/acs.jctc.5b00935.

[33] B.R. Brooks, C.L. Brooks, A.D. Mackerell, L. Nilsson, R.J. Petrella, B. Roux, Y. Won, G. Archontis, C. Bartels, S. Boresch, A. Caflisch, L. Caves, Q. Cui, A.R. Dinner, M. Feig, S. Fischer, J. Gao, M. Hodoscek, W. Im, K. Kuczera, T. Lazaridis, J. Ma, V. Ovchinnikov, E. Paci, R.W. Pastor, C.B. Post, J.Z. Pu, M. Schaefer, B. Tidor, R.M. Venable, H.L. Woodcock, X. Wu, W. Yang, D.M. York, M. Karplus, CHARMM: The biomolecular simulation program, J. Comput. Chem. 30 (2009) 1545–1614. doi:10.1002/jcc.21287.

[34] S. Jo, T. Kim, V.G. Iyer, W. Im, CHARMM-GUI: A web-based graphical user interface for CHARMM, J. Comput. Chem. 29 (2008) 1859–1865. doi:10.1002/jcc.20945.

[35] J. Huang, S. Rauscher, G. Nawrocki, T. Ran, M. Feig, B.L. De Groot, H. Grubmüller, A.D. MacKerell, CHARMM36m: An improved force field for folded and intrinsically disordered proteins, Nat. Methods. 14 (2016) 71–73. doi:10.1038/nmeth.4067.

[36] W.L. Jorgensen, J. Chandrasekhar, J.D. Madura, R.W. Impey, M.L. Klein, Comparison of simple potential functions for simulating liquid water, J. Chem. Phys. 79 (1983) 926–935. doi:10.1063/1.445869.

[37] R. Fletcher, M.J.D. Powell, A Rapidly Convergent Descent Method for Minimization, Comput. J. 6 (1963) 163–168. doi:10.1093/comjnl/6.2.163.

[38] G. Bussi, D. Donadio, M. Parrinello, Canonical sampling through velocity rescaling, J. Chem. Phys. 126 (2007). doi:10.1063/1.2408420.

[39] H.J.C. Berendsen, J.P.M. Postma, W.F. Van Gunsteren, A. Dinola, J.R. Haak, Molecular dynamics with coupling to an external bath, J. Chem. Phys. 81 (1984) 3684–3690. doi:10.1063/1.448118.

[40] D.J. Evans, B.L. Holian, The Nose-Hoover thermostat, J. Chem. Phys. 83 (1985) 4069–4074. doi:10.1063/1.449071.

[41] T. Darden, D. York, L. Pedersen, Particle mesh Ewald: An N·log(N) method for Ewald sums in large systems, J. Chem. Phys. 98 (1993) 10089–10092. doi:10.1063/1.464397.

[42] M.J. Abraham, T. Murtola, R. Schulz, S. Páll, J.C. Smith, B. Hess, E. Lindah, Gromacs: High performance molecular simulations through multi-level parallelism from laptops to supercomputers, SoftwareX. 1–2 (2015) 19–25. doi:10.1016/j.softx.2015.06.001.

[43] W.J. Allen, J.A. Lemkul, D.R. Bevan, GridMAT-MD: A grid-based membrane analysis tool for use with molecular dynamics, J. Comput. Chem. 30 (2009) 1952–1958. doi:10.1002/jcc.21172.

[44] G. Khelashvili, B. Kollmitzer, P. Heftberger, G. Pabst, D. Harries, Calculating the bending modulus for multicomponent lipid membranes in different thermodynamic phases, J. Chem. Theory Comput. 9 (2013) 3866–3871. doi:10.1021/ct400492e.

[45] G. Khelashvili, G. Pabst, D. Harries, Cholesterol orientation and tilt modulus in DMPC bilayers, J. Phys. Chem. B. 114 (2010) 7524–7534. doi:10.1021/jp101889k.

[46] L. Janosi, A.A. Gorfe, Simulating POPC and POPC/POPG bilayers: Conserved packing and altered surface reactivity, J. Chem. Theory Comput. 6 (2010) 3267–3273. doi:10.1021/ct100381g.

[47] E. Plesnar, W.K. Subczynski, M. Pasenkiewicz-Gierula, Saturation with cholesterol increases vertical order and smoothes the surface of the phosphatidylcholine bilayer: A molecular simulation study, Biochim. Biophys. Acta - Biomembr. 1818 (2012) 520–529. doi:10.1016/j.bbamem.2011.10.023.

[48] R.M. Venable, F.L.H. Brown, R.W. Pastor, Mechanical properties of lipid bilayers from molecular dynamics simulation, Chem. Phys. Lipids. 192 (2015) 60–74. doi:10.1016/j.chemphyslip.2015.07.014.

[49] G. Grasso, S. Muscat, M. Rebella, U. Morbiducci, A. Audenino, A. Danani, M.A. Deriu, Cell penetrating peptide modulation of membrane biomechanics by Molecular dynamics, J. Biomech. 73 (2018) 137–144. doi:10.1016/j.jbiomech.2018.03.036.

[50] A. Hossein, M. Deserno, Spontaneous Curvature, Differential Stress, and Bending Modulus of Asymmetric Lipid Membranes, Biophys. J. 118 (2020) 624–642. doi:10.1016/j.bpj.2019.11.3398.

[51] D. Bochicchio, L. Monticelli, The membrane bending modulus in experiments and simulations: A puzzling picture, in: Adv. Biomembr. Lipid Self-Assembly, 2016: pp. 117–143. doi:10.1016/bs.abl.2016.01.003.

[52] B.C. Borro, L. Parolini, P. Cicuta, V. Foderà, L. Di Michele, Interaction with prefibrillar species and amyloid-like fibrils changes the stiffness of lipid bilayers, Phys. Chem. Chem. Phys. 19 (2017) 27930–27934. doi:10.1039/c7cp05339h.

[53] H.W. Querfurth, F.M. LaFerla, Alzheimer's disease, N. Engl. J. Med. 362 (2010) 329–344. doi:10.1056/NEJMra0909142.

[54] T. Iwatsubo, A. Odaka, N. Suzuki, H. Mizusawa, N. Nukina, Y. Ihara, Visualization of Aβ42(43) and Aβ40 in senile plaques with end-specific Aβ monoclonals: Evidence that an initially deposited species is Aβ42(43), Neuron. 13 (1994) 45–53. doi:10.1016/0896-6273(94)90458-8.

[55] H.A. Lashuel, H. Hirling, Rescuing defective vesicular trafficking protects against alpha-synuclein toxicity in cellular and animal models of Parkinson's disease., ACS Chem. Biol. 1 (2006) 420–424. doi:10.1021/cb600331e.

[56] E.E. Ambroggio, D.H. Kim, F. Separovic, C.J. Barrow, K.J. Barnham, L.A. Bagatolli, G.D. Fidelio, Surface behavior and lipid interaction of Alzheimer β-amyloid peptide 1-42: A membrane-disrupting peptide, Biophys. J. 88 (2005) 2706–2713. doi:10.1529/biophysj.104.055582.

[57] J.A. McLaurin, A. Chakrabartty, Characterization of the interactions of Alzheimer β-amyloid peptides with phospholipid membranes, Eur. J. Biochem. 245 (1997) 355–363. doi:10.1111/j.1432-1033.1997.t01-2-00355.x.

[58] R. Oropesa-Nuñez, S. Seghezza, S. Dante, A. Diaspro, R. Cascella, C. Cecchi, M. Stefani, F. Chiti, C. Canale, Interaction of toxic and non-toxic HypF-N oligomers with lipid bilayers investigated at high resolution with atomic force microscopy, Oncotarget. 7 (2016) 44991–45004. doi:10.18632/oncotarget.10449.

[59] E.Y. Chi, S.L. Frey, A. Winans, K.L.H. Lam, K. Kjaer, J. Majewski, K.Y.C. Lee, Amyloid-beta fibrillogenesis seeded by interface-induced peptide misfolding and self-assembly., Biophys. J.

98 (2010) 2299–2308. doi:10.1016/j.bpj.2010.01.056.

[60] C. Aisenbrey, T. Borowik, R. Byström, M. Bokvist, F. Lindström, H. Misiak, M.A. Sani, G. Gröbner, How is protein aggregation in amyloidogenic diseases modulated by biological membranes?, Eur. Biophys. J. 37 (2008) 247–255. doi:10.1007/s00249-007-0237-0.

[61] C.M. Yip, J. McLaurin, Amyloid-β peptide assembly: A critical step in fibrillogenesis and membrane disruption, Biophys. J. 80 (2001) 1359–1371. doi:10.1016/S0006-3495(01)76109-7.

[62] L.N. Zhao, H. Long, Y. Mu, L.Y. Chew, The toxicity of amyloid β oligomers, Int. J. Mol. Sci. 13 (2012) 7303–7327. doi:10.3390/ijms13067303.

[63] X. Yu, Q. Wang, Q. Pan, F. Zhou, J. Zheng, Molecular interactions of Alzheimer amyloid-β oligomers with neutral and negatively charged lipid bilayers, Phys. Chem. Chem. Phys. 15 (2013) 8878–8889. doi:10.1039/c3cp44448a.

[64] C.H. Davis, M.L. Berkowitz, A molecular dynamics study of the early stages of amyloid-β(1-42) oligomerization: The role of lipid membranes, Proteins Struct. Funct. Bioinforma. 78 (2010) 2533–2545. doi:10.1002/prot.22763.

[65] F. Chiti, C.M. Dobson, Protein Misfolding, Functional Amyloid, and Human Disease, Annu. Rev. Biochem. 75 (2006) 333–366. doi:10.1146/annurev.biochem.75.101304.123901.

[66] F. Chiti, C.M. Dobson, Amyloid formation by globular proteins under native conditions, Nat. Chem. Biol. 5 (2009) 15–22. doi:10.1038/nchembio.131.

[67] J. Frackowiak, A. Zoltowska, H.M. Wisniewski, Non-fibrillar β-amyloid protein is associated with smooth muscle cells of vessel walls in alzheimer disease, J. Neuropathol. Exp. Neurol. 53 (1994) 637–645. doi:10.1097/00005072-199411000-00011.

[68] Y. Gong, L. Chang, K.L. Viola, P.N. Lacor, M.P. Lambert, C.E. Finch, G.A. Krafft, W.L. Klein, Alzheimer's disease-affected brain: Presence of oligomeric Aβ ligands (ADDLs) suggests a molecular basis for reversible memory loss, Proc. Natl. Acad. Sci. U. S. A. 100 (2003) 10417–10422. doi:10.1073/pnas.1834302100.

[69] R. Kayed, E. Head, J.L. Thompson, T.M. McIntire, S.C. Milton, C.W. Cotman, C.G. Glabel, Common structure of soluble amyloid oligomers implies common mechanism of pathogenesis, Science (80-.). 300 (2003) 486–489. doi:10.1126/science.1079469.

[70] A. Noguchi, S. Matsumura, M. Dezawa, M. Tada, M. Yanazawa, A. Ito, M. Akioka, S. Kikuchi, M. Sato, M. Noda, A. Fukunari, S.I. Muramatsu, Y. Itokazu, K. Sato, H. Takahashi, D.B. Teplow, Y.I. Nabeshima, A. Kakita, K. Imahori, M. Hoshi, Isolation and characterization of patient-derived, toxic, high mass Amyloid β-protein (Aβ) assembly from Alzheimer disease brains, J. Biol. Chem. 284 (2009) 32895–32905. doi:10.1074/jbc.M109.000208.

[71] E. Pham, L. Crews, K. Ubhi, L. Hansen, A. Adame, A. Cartier, D. Salmon, D. Galasko, S. Michael, J.N. Savas, J.R. Yates, C. Glabe, E. Masliah, Progressive accumulation of amyloid-β oligomers in Alzheimer's disease and in amyloid precursor protein transgenic mice is accompanied by selective alterations in synaptic scaffold proteins, FEBS J. 277 (2010) 3051–3067. doi:10.1111/j.1742-4658.2010.07719.x.

[72] M. Ohno, L. Chang, W. Tseng, H. Oakley, M. Citron, W.L. Klein, R. Vassar, J.F. Disterhoft, Temporal memory deficits in Alzheimer's mouse models: Rescue by genetic deletion of BACE1, Eur. J. Neurosci. 23 (2006) 251–260. doi:10.1111/j.1460-9568.2005.04551.x.

[73] N. Kučerka, S. Tristram-Nagle, J.F. Nagle, Structure of fully hydrated fluid phase lipid bilayers with monounsaturated chains, J. Membr. Biol. 208 (2006) 193–202. doi:10.1007/s00232-005-

7006-8.

[74] D.E. Elmore, Molecular dynamics simulation of a phosphatidylglycerol membrane, FEBS Lett. 580 (2006) 144–148. doi:10.1016/j.febslet.2005.11.064.

[75] J.F. Nagle, Experimentally determined tilt and bending moduli of single-component lipid bilayers, Chem. Phys. Lipids. 205 (2017) 18–24. doi:10.1016/j.chemphyslip.2017.04.006.

[76] F. Bemporad, F. Chiti, Protein misfolded oligomers: Experimental approaches, mechanism of formation, and structure-toxicity relationships, Chem. Biol. 19 (2012) 315–327. doi:10.1016/j.chembiol.2012.02.003.

[77] S. Campioni, B. Mannini, M. Zampagni, A. Pensalfini, C. Parrini, E. Evangelisti, A. Relini, M. Stefani, C.M. Dobson, C. Cecchi, F. Chiti, A causative link between the structure of aberrant protein oligomers and their toxicity, Nat. Chem. Biol. 6 (2010) 140–147. doi:10.1038/nchembio.283.

[78] C. Cecchi, M. Stefani, The amyloid-cell membrane system. The interplay between the biophysical features of oligomers/fibrils and cell membrane defines amyloid toxicity, Biophys. Chem. 182 (2013) 30–43. doi:10.1016/j.bpc.2013.06.003.

[79] M. Serra-Batiste, J. Tolchard, F. Giusti, M. Zoonens, N. Carulla, Stabilization of a membrane-associated amyloid-β oligomer for its validation in Alzheimer's disease, Front. Mol. Biosci. 5 (2018). doi:10.3389/fmolb.2018.00038.

[80] T.L. William, B.R.G. Johnson, B. Urbanc, A.T.A. Jenkins, S.D.A. Connell, L.C. Serpell, Aβ42 oligomers, but not fibrils, simultaneously bind to and cause damage to ganglioside-containing lipid membranes, Biochem. J. 439 (2011) 67–77. doi:10.1042/BJ20110750.

[81] I. Benilova, E. Karran, B. De Strooper, The toxic Aβ oligomer and Alzheimer's disease: An emperor in need of clothes, Nat. Neurosci. 15 (2012) 349–357. doi:10.1038/nn.3028.

[82] F. Tofoleanu, N.V. Buchete, Molecular interactions of Alzheimer's Aβ protofilaments with lipid membranes, J. Mol. Biol. 421 (2012) 572–586. doi:10.1016/j.jmb.2011.12.063.

[83] L. Connelly, H. Jang, F. Teran Arce, R. Capone, S.A. Kotler, S. Ramachandran, B.L. Kagan, R. Nussinov, R. Lal, Atomic force microscopy and MD simulations reveal pore-like structures of all-d-enantiomer of Alzheimer's β-amyloid peptide: Relevance to the ion channel mechanism of AD pathology, J. Phys. Chem. B. 116 (2012) 1728–1735. doi:10.1021/jp2108126.

[84] C. Liu, M. Zhao, L. Jiang, P.N. Cheng, J. Park, M.R. Sawaya, A. Pensalfini, D. Gou, A.J. Berk, C.G. Glabe, J. Nowick, D. Eisenberg, Out-of-register β-sheets suggest a pathway to toxic amyloid aggregates, Proc. Natl. Acad. Sci. U. S. A. 109 (2012) 20913–20918. doi:10.1073/pnas.1218792109.

[85] T.D. Do, N.E. Lapointe, R. Nelson, P. Krotee, E.Y. Hayden, B. Ulrich, S. Quan, S.C. Feinstein, D.B. Teplow, D. Eisenberg, J.E. Shea, M.T. Bowers, Amyloid β-Protein C-Terminal Fragments: Formation of Cylindrins and β-Barrels, J. Am. Chem. Soc. 138 (2016) 549–557. doi:10.1021/jacs.5b09536.

[86] D.C. Bode, M. Freeley, J. Nield, M. Palma, J.H. Viles, Amyloid-β oligomers have a profound detergent-like effect on lipid membrane bilayers, imaged by atomic force and electron microscopy, J. Biol. Chem. 294 (2019) 7566–7572. doi:10.1074/jbc.AC118.007195.

[87] M.F.M. Sciacca, C. Tempra, F. Scollo, D. Milardi, C. La Rosa, Amyloid growth and membrane damage: Current themes and emerging perspectives from theory and experiments on Aβ and hIAPP, Biochim. Biophys. Acta - Biomembr. 1860 (2018) 1625–1638.

doi:10.1016/j.bbamem.2018.02.022.